Reverse Osmosis Separations of Polyethylene Glycols in Dilute Aqueous Solutions Using Porous Cellulose Acetate Membranes

FU-HUNG HSIEH, TAKESHI MATSUURA, and S. SOURIRAJAN,
Division of Chemistry, National Research Council of Canada, Ottawa, Canada K1A OR9

Synopsis

Reverse osmosis separations of eight polyethylene glycol (PEG) solutes in the average molecular weight range of 200 to 6750 in single-solute dilute aqueous solutions have been studied using porous cellulose acetate membranes at the operating pressures of 50, 75, and 100 psig. Diffusivity data for the above PEG solutes have also been obtained from experimental data on intrinsic viscosities. From an analysis of all experimental data, numerical values for the parameters representing the polar ($-\Delta\Delta G/RT$), steric ($\delta^*\Sigma E_s$), and nonpolar ($\omega^*\Sigma s^*$) forces governing reverse osmosis separations of PEG solutes have been generated. These numerical values are useful for precise characterization of cellulose acetate membranes for whose specifications sodium chloride is not the appropriate reference solute because of its low or practically negligible separation under reverse osmosis operating conditions. This work also illustrates that solute separation in reverse osmosis can predictably increase or decrease with increase in operating pressure depending on experimental conditions.

INTRODUCTION

The polyethylene glycols are linear polymers of ethylene oxide terminated at both ends by hydroxyl groups. They have the general formula

$$HO(CH_2CH_2O)_n\ CH_2CH_2OH$$

where n represents the number of oxyethylene repeat units in the polymer molecule. A study of the reverse osmosis separations of polyethylene glycol solutes in dilute aqueous solutions using porous cellulose acetate membranes is of both fundamental and practical interest. Cellulose acetate material has already been shown to behave as a net proton acceptor (base) with respect to solute–membrane material interactions in reverse osmosis systems involving aqueous solutions.[1] Since ether linkages have a net basic character, and Taft's polar parameter for ethylene glycol is negative ($\sigma^* = -0.200$), water may be expected to be preferentially sorbed at the membrane–solution interface in reverse osmosis systems involving aqueous solutions of polyethylene glycol and porous cellulose acetate membranes.[2,3] Further, since reverse osmosis separations in such systems are governed by the polar, steric, and nonpolar forces prevailing at the membrane–solution interface, the experimental reverse osmosis data can be analyzed on the basis of already established transport equations involving parameters representing the effects of the above forces on membrane performance.[3–6] Such analysis could lead to general methods of analyzing reverse osmosis data involving polymer solutes, which is of fundamental interest in reverse osmosis transport. Since reverse osmosis separations of polymer solutes

Journal of Applied Polymer Science, Vol. 23, 561–573 (1979)

0021-8995/79/0023-0561$01.00

involve membranes with relatively bigger average size of pores on the membrane surface (compared to membranes used for separation of ionic solutes), the above analysis could also lead to practical methods of specifying such membranes in terms of reverse osmosis data for appropriate polymer solutes in sufficiently dilute aqueous solutions. The development of such methods is particularly useful with respect to cellulose acetate membranes for whose specifications sodium chloride is not the most suitable reference solute because of its low or practically negligible separation under reverse osmosis operating conditions. Hence, the object of this work is to analyze data on reverse osmosis separations of polyethylene glycol solutes in dilute aqueous solutions at low operating pressures (100 psig or less) using porous cellulose acetate membranes of different surface porosities and generate the numerical values for the parameters[5,6] representing the polar ($-\Delta\Delta G/RT$), steric ($\delta^*\Sigma E_s$), and nonpolar ($\omega^*\Sigma s^*$) effects for reverse osmosis systems involving polyethylene glycol solutes of different molecular weights.

EXPERIMENTAL

Eight polyethylene glycols (BDH Chemicals) in the average molecular weight range of 200 to 6000 (designated as PEG number representing approximate average molecular weight), reagent-grade sodium chloride, and flat cellulose acetate membranes of different surface porosities made in the laboratory by the method described by Kutowy et al.[7] were used in this work. All membranes were initially subjected to a pure water pressure of 150 psig for 3 hr prior to reverse osmosis experiments to stabilize their porous structure. The specifications[8] of the membranes used are given in Table I in terms of pure water permeability constant A (in g-mole of H_2O/cm^2 sec atm), and solute transport parameter $D_{AM}/K\delta$ (in cm/sec, treated as a single quantity for purposes of analysis) for sodium chloride at 100 psig. An aqueous feed solution containing 5800 ppm of NaCl was used for obtaining data on membrane specifications.

All experiments were carried out at the laboratory temperature (23–25°C) in the apparatus shown in Figure 2 in reference 3. The operating pressure for the

TABLE I
Specifications and Some Performance Data for the Cellulose Acetate Membranes Used[a]

	Film no.				
	1	2	3	4	5
Pure water permeability constant A, $\left(\frac{\text{g - mole } H_2O}{\text{cm}^2 \text{ sec atm}}\right)$ $\times 10^{6}$ [b]	4.916	8.523	9.165	10.62	17.29
Solute transport parameter $\left(\frac{D_{AM}}{K\delta}\right)_{NaCl}$, (cm/sec) $\times 10^4$	11.11	41.52	42.21	61.07	126.3
$\ln C^*_{NaCl}$	−8.17	−6.85	−6.82	−6.42	−5.74
Solute separation, %	31.3	16.9	16.4	12.5	8.0
Product rate, g/hr[c]	25.41	47.51	49.93	58.17	93.18

[a] Feed concentration, 5800 ppm NaCl.
[b] Operating pressure, 100 psig.
[c] Area of film surface, 13.2 cm^2.

reverse osmosis experiments was in the range 50 to 100 psig. Unless otherwise specified, the concentration of polyethylene glycol in the feed was about 50 ppm, and the feed flow rate was 530 ± 10 cm^3/min, corresponding to a mass transfer coefficient k in the range of 16.0×10^{-4} to 30×10^{-4} cm/sec for a 5800-ppm NaCl–H_2O reference feed solution. In each experiment the pure water permeation rate PWP and the membrane permeated product rate PR in g/hr per given area of membrane surface (= 13.2 cm^2 in this work) were determined. Data on PWP and PR were essentially the same in all experiments, showing thereby that the osmotic pressure effects on reverse osmosis transport could be considered negligible under the experimental conditions used. The fraction solute separation f in each experiment was obtained from the relation

$$f = \frac{\text{solute ppm in feed} - \text{solute ppm in product}}{\text{solute ppm in feed}}$$

The analysis for sodium chloride in aqueous solutions was done using a conductivity bridge. A Beckman total carbon analyzer Model 915 was used to measure the concentrations of polyethylene glycol in feed and product solutions. In the latter case, a calibration curve was always prepared just prior to analysis.

RESULTS AND DISCUSSION

Diffusivity Data for Polyethylene Glycols in Dilute Aqueous Solutions

The diffusivity D_{AB} of a polymer solute at infinite dilution is related to its molecular friction coefficient f_0 by the Einstein equation[9,10] expressed in the form

$$D_{AB} = kT/f_0 \tag{1}$$

where k is the Boltzmann constant and T is the absolute temperature (in °K). The value of f_0 depends on the size and shape of the solute molecule as well as the viscosity η_0 of the surrounding solvent (water). For a flexible-chain molecule such as polyethylene glycol in dilute solution, f_0 is related to the molecular weight M of the solute and the intrinsic viscosity $[\eta]$ of the solution by the relation[11]

$$f_0/\eta_0 = p\phi^{-1/3}(M[\eta])^{1/3} \tag{2}$$

where p and ϕ are universal constants applicable for all polymers. Mandelkern and Flory[11] have experimentally determined that $p^{-1}\phi^{1/3} \cong 2.5 \times 10^6$. Therefore, combining eqs. (1) and (2),

$$D_{AB} = 2.5 \times 10^6 kT/\{\eta_0(M[\eta])^{1/3}\} \tag{3}$$

Using data on η_0 and $[\eta]$ obtained experimentally, the values of D_{AB} for the polyethylene glycol solutes used in this work were calculated from eq. (3), and the results obtained are given in Table II.

TABLE II
Some Physiochemical Data for Polyethylene Glycols

Solute	$\bar{M}_w$	n[a]	$[\eta]$, dl/g	D_{AB}, (cm²/sec) × 10⁶	$\left(\frac{-\Delta\Delta G}{RT}\right)$	$\delta^*\Sigma E_s$	$\omega^*\Sigma s^*$	$\left(\frac{-\Delta\Delta G}{RT}\right) + \delta^*\Sigma E_s + \omega^*\Sigma s^*$
PEG-200	200	3.1	0.0300	6.33	7.14	−6.25	0	0.89
PEG-300	300	5.4	0.0352	5.24	8.76	−8.23	0	0.53
PEG-400	400	7.7	0.0383	4.63	10.42	−10.21	0	0.21
PEG-600	600	12.2	0.0430	3.89	13.59	−14.08	0	−0.49
PEG-1000	1000	21.3	0.0516	3.09	20.02	−21.90	0.85	−1.03
PEG-1500	1500	32.6	0.0693	2.45	28.07	−31.61	1.92	−1.62
PEG-4000	3650	81.3	0.1040	1.59	62.56	−73.49	8.33	−2.60
PEG-6000	6750	152	0.2430	0.976	111.70	−134.30	18.80	−3.80

[a] $n = \dfrac{\text{average molecular weight} - \text{molecular weight of nonrepeating unit}}{\text{molecular weight of repeating unit.}}$

Experimental Determination of Solute Transport Parameter for Polyethylene Glycols

Using experimental data on PR and f, the solute transport parameter $D_{AM}/K\delta$ (in cm/sec) for the polyethylene glycol-solute used was calculated in each experiment from the following relations applicable for dilute feed solutions:

$$(D_{AM}/K\delta) = \frac{PR}{3600S\rho}\frac{1-f}{f}\left[\exp\left(\frac{PR}{3600Sk\rho}\right)\right]^{-1} \tag{4}$$

and

$$k = k_{\mathrm{NaCl}}\,[D_{AB}/(D_{AB})_{\mathrm{NaCl}}]^{2/3} \tag{5}$$

where S = effective area of membrane surface (= 13.2 cm² in this work); ρ = density of solution (≈ that of pure water); k = mass transfer coefficient for the polyethylene glycol solute on the high-pressure side of the membrane; k_{NaCl} = corresponding mass transfer coefficient for the NaCl for a 5800 ppm NaCl–H_2O feed solution, obtained from the application of the basic Kimura-Sourirajan transport equations[8]; and D_{AB} and $(D_{AB})_{\mathrm{NaCl}}$ refer to diffusivities of solute (Table II) and NaCl (= 1.61×10^{-5} cm²/sec), respectively. Equations (4) and (5) have been derived.[12]

With respect to cellulose acetate membranes, it has already been shown[8,13] that the values of $D_{AM}/K\delta$ for several inorganic and organic solutes are independent of solute concentration in the feed solution. In order to test whether that is the case with respect of PEG solutes also, the values of $D_{AM}/K\delta$ for the PEG-6000 solute in the concentration range of 50 to 200 ppm were experimentally determined at the operating pressure of 100 psig using five membranes of different surface porosities. The results obtaind, shown in Figure 1, confirmed that the values of $D_{AM}/K\delta$ were indeed independent of feed concentration for each one of the films tested. On the basis of this result, it is reasonable to assume that a similar correlation exists for all the other lower molecular weight PEG solutes also studied in this work.

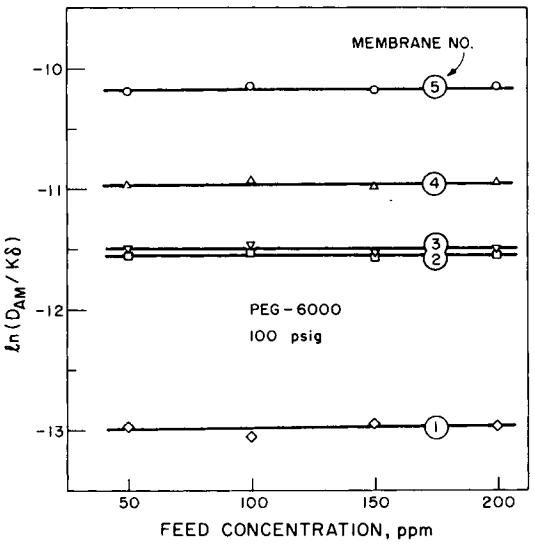

Fig. 1. Effect of feed concentration on solute transport parameter for PEG-6000 at 100 psig.

Analysis of Experimental Data on $D_{AM}/K\delta$

The solute transport parameter $D_{AM}/K\delta$ for nonionized polar aliphatic and alicyclic organic solutes in aqueous solutions, whose reverse osmosis separations are governed by polar, steric, and nonpolar effects *and* preferential sorption of water at the membrane–solution interface, is given by the general expression[5,6]

$$\ln (D_{AM}/K\delta) = \ln C^*_{NaCl} + \ln \Delta^* + \left(-\frac{\Delta\Delta G}{RT}\right) + \delta^* \Sigma E_s + \omega^* \Sigma s^* \qquad (6)$$

Referring to the right side of eq. (6), the quantity $\ln C^*_{NaCl}$ expresses the porous structure of the membrane surface in terms of $D_{AM}/K\delta$ for NaCl and the data on free-energy parameters ($-\Delta\Delta G/RT$) for Na^+ and Cl^- ions, which are characteristic of the chemical nature of the material of the membrane surface but independent of its porous structure. The values of $-\Delta\Delta G/RT$ for Na^+ and Cl^- ions for the cellulose acetate material used in this work are 5.79 and −4.42, respectively.[14] Using these values and those for $D_{AM}/K\delta$ given by data on membrane specifications (Table I), the values of $\ln C^*_{NaCl}$ can be calculated from the relation[14]

$$\ln C^*_{NaCl} = \ln (D_{AM}/K\delta)_{NaCl} - \left[\left(-\frac{\Delta\Delta G}{RT}\right)_{Na^+} + \left(-\frac{\Delta\Delta G}{RT}\right)_{Cl^-}\right] \qquad (7)$$

The values of $\ln C^*_{NaCl}$ so calculated for the membranes used in this work were in the range of −8.17 to −5.74 (Table I).

The quantity $\ln \Delta^*$ is a scale factor and is a function of $\ln C^*_{NaCl}$ only; the correlation of $\ln \Delta^*$ with $\ln C^*_{NaCl}$ has been experimentally established for cellulose acetate membranes as given in Figure 3 in reference 5. According to this correlation, the value of $\ln \Delta^* = -0.92$ for all values of $\ln C^*_{NaCl}$ greater than −9.6, which is the case for all the membranes used in this work.

The quantity $-\Delta\Delta G/RT$ represents the free-energy parameter for the PEG solute under consideration, which can be computed from the following relations[5]:

$$\Delta G_B = \Sigma\gamma_B \text{ (structural group)} + \gamma_{B,0} \tag{8}$$

$$\Delta G_I = \Sigma\gamma_I \text{ (structural group)} + \gamma_{I,0} \tag{9}$$

and

$$-\frac{\Delta\Delta G}{RT} = -\frac{1}{RT}(\Delta G_I - \Delta G_B) \tag{10}$$

where ΔG represents the free energy of hydration of solute; γ (structural group) represents the structural group contribution to ΔG; the subscripts I and B represent the membrane–solution interface and the bulk solution phase, respectively; the quantities $\gamma_{B,0}$ and $\gamma_{I,0}$ are characteristic constants; R is gas constant; and T is absolute temperature. The numerical values of γ_B for the structural groups $>CH_2$, $-OH$, and $>O$ are 0.17, 3.99, and -4.03, respectively; the corresponding applicable values of γ_I are 0.24, 17.04, and -4.59, respectively. Further, $\gamma_{B,0} = -12.04$, $\gamma_{I,0} = -41.21$, and RT at 25°C = 0.5925. Using the above data,[5] the numerical values of $-\Delta\Delta G/RT$ for all the PEG solutes studied in this work were computed, and the results obtained are given in Table I; again, these values of $-\Delta\Delta G/RT$ are independent of the porous structure of the membrane surface.

The quantities $\delta^*\Sigma E_s$ and $\omega^*\Sigma s^*$ in eq. (6) represent the total effect of steric and nonpolar forces prevailing at the membrane–solution interface. The magnitude of these quantities for different PEG solutes can be determined from their experimental $D_{AM}/K\delta$ data as follows.

The modified Small's number Σs^* in the term representing the total nonpolar effect ($\omega^*\Sigma s^*$) is related to the solubility of the solute in water[15]; the value of Σs^* decreases with increase in solubility. Since the PEG solutes in the molecular weight range of 200 to 600 are completely water soluble, their Σs^* value may be assumed to be zero, so that the quantity $\omega^*\Sigma s^* = 0$ for such solutes. Therefore, for the four solutes PEG-200, PEG-300, PEG-400, and PEG-600, the magnitude of the quantity $\delta^*\Sigma E_s$ representing the steric effect can be determined from experimental $D_{AM}/K\delta$ data and eq. (6) from the relation

$$\delta^*\Sigma E_s = \ln (D_{AM}/K\delta) - \ln C^*_{NaCl} - \ln \Delta^* - (-\Delta\Delta G/RT) \tag{11}$$

The values of $\delta^*\Sigma E_s$ so calculated are plotted in Figure 2 for five membranes of different surface porosities at the operating pressures of 50, 75, and 100 psig. The results showed that for each solute the quantity $\delta^*\Sigma E_s$ was essentially a constant independent of operating pressure and the porous structure of the membrane surface in the range of ln C^*_{NaCl} values used in this work. The observed effect of operating pressure on $\delta^*\Sigma E_s$ (Fig. 2) is consistent with earlier work.[5] The constancy of $\delta^*\Sigma E_s$ for membranes of different surface porosities (Fig. 2) arises from the fact that the change in the values of δ^* for alcohols and ethers with change in average pore size on the membrane surface is essentially negligible for ln C^*_{NaCl} values greater than -9.6, which is the case for all the membranes used in this work.

The average value of the quantity $\delta^*\Sigma E_s$ obtained for each of the four PEG solutes PEG-200, PEG-300, PEG-400, and PEG-600 from data given in Figure 2 can be analyzed further. The total steric effect, represented by the quantity $\delta^*\Sigma E_s$, may be considered to be the sum of that contributed by the nonrepeating unit, $\delta^*\Sigma E_s(OHCH_2CH_2OH)$, and n times of that contributed by the repeating unit, $\delta^*\Sigma E_s(CH_2CH_2O)$, in the molecular structure of the PEG solute $HO-(CH_2CH_2O)_nCH_2CH_2OH$, so that

$$\delta^*\Sigma E_s = n[\delta^*\Sigma E_s(CH_2CH_2O)] + \delta^*\Sigma E_s(OHCH_2CH_2OH) \tag{12}$$

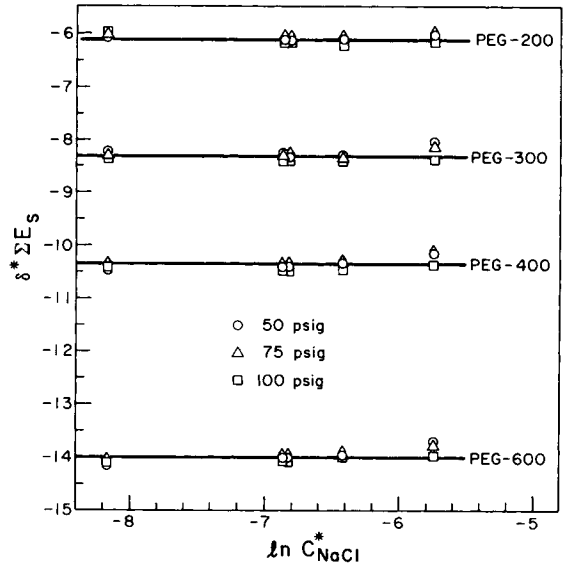

Fig. 2. Effect of surface porosity of membrane on total steric effect of various polyethylene glycol solutes: (○) 50 psig; (△) 75 psig; (□) 100 psig.

Hence, the values of $\delta^*\Sigma E_s$ obtained experimentally for the four PEG solutes (Figure 2) were subjected to regression analysis to determine the component contributions $\delta^*\Sigma E_s$ (CH_2CH_2O) and $\delta^*\Sigma E_s$ ($OHCH_2CH_2OH$), which gave the following data:

$$\delta^*\Sigma E_s(CH_2CH_2O) = -0.860 \tag{13}$$

and

$$\delta^*\Sigma E_s(OHCH_2CH_2OH) = -3.585 \tag{14}$$

Using the above data, the values of $\delta^*\Sigma E_s$ representing the total steric effect were computed for all the eight PEG solutes studied in this work, and the results obtained are given in Table II.

Referring again to the terms on the right side of eq. (6), all the quantities are now known except $\omega^*\Sigma s^*$, representing the nonpolar effect of $D_{AM}/K\delta$ for the solute. The magnitude of $\omega^*\Sigma s^*$ has already been set equal to zero with respect to solutes PEG-200, PEG-300, PEG-400, and PEG-600. Using experimental $D_{AM}/K\delta$ data, the values of $\omega^*\Sigma s^*$ for the solutes PEG-1000, PEG-1500, PEG-4000, and PEG-6000 can then be calculated from eq. (6), which can be rewritten as follows:

$$\omega^*\Sigma s^* = \ln (D_{AM}/K\delta) - \ln C^*_{NaCl} - \ln \Delta^* - \left(-\frac{\Delta\Delta G}{RT}\right) - \delta^*\Sigma E_s \tag{15}$$

The values of $\omega^*\Sigma s^*$ so calculated from data on $D_{AM}/K\delta$ obtained with five membranes of different surface porosities at different operating pressures are plotted in Figure 3, which shows that the above values are essentially constants characteristic of the solutes but independent of operating pressures and porous structure of the membrane surface. Such correlation of $\omega^*\Sigma s^*$ is consistent with its nature and confirms the observations made earlier with respect to higher alcohol solutes.[6] The average value of $\omega^*\Sigma s^*$ for each PEG solute obtained from

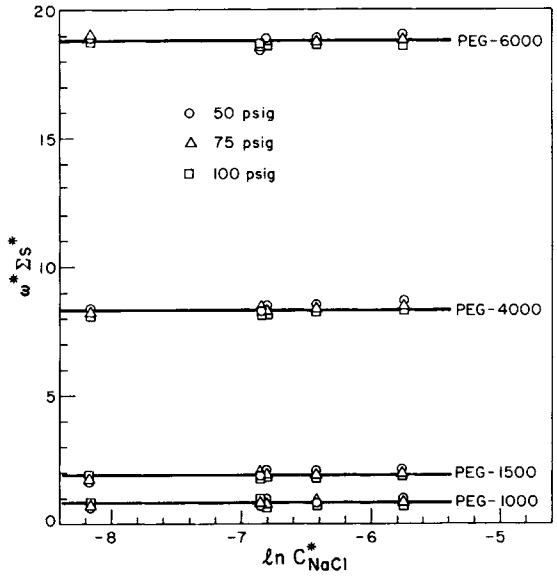

Fig. 3. Effect of surface porosity of membrane on total nonpolar effect of various polyethylene glycol solutes: (○) 50 psig; (△) 75 psig; (□) 100 psig.

the experimental data given in Figure 3 is listed in Table II. This table shows that the values of the parameters representing the polar ($-\Delta\Delta G/RT$) and nonpolar ($\omega^*\Sigma s^*$) effects increase and that the values of $\delta^*\Sigma E_s$ representing the steric effect decrease with increase in the molecular weight of the PEG solute.

The change in $\omega^*\Sigma s^*$ is understandable on the basis of the effect of molecular structure on the molar solubility of the solute.[15] The change in the polar ($-\Delta\Delta G/RT$) and steric ($\delta^*\Sigma E_s$) effects represents the cumulative effect of the numerical values assigned to the structural components in the molecule. While increases in the values of $-\Delta\Delta G/RT$ and $\omega^*\Sigma s^*$ tend to increase the attraction of the solute toward the membrane surface, decrease in the values of $\delta^*\Sigma E_s$ tends to increase solute repulsions at the membrane–solution interface; the net effect is governed by the resultant of the sum of the quantities representing the polar, steric, and nonpolar effects ($-\Delta\Delta G/RT + \delta^*\Sigma E_s + \omega^*\Sigma s^*$). Since this sum (Table II) decreases with increase in molecular weight of PEG, one may conclude that solute repulsion and hence preferential sorption of water at the membrane–solution interface increase with increase in molecular weight of PEG solute in the molecular weight range studied in this work.

Predictability of Reverse Osmosis Separations of PEG Solutes in Dilute Aqueous Solutions at Low Operating Pressures

The data on $-\Delta\Delta G/RT$, $\delta^*\Sigma E_s$, and $\omega^*\Sigma s^*$ for PEG solutes generated above (Table II) offer a means of predicting reverse osmosis separations of these solutes from data on membrane specifications given in terms of A and $(D_{AM}/K\delta)_{NaCl}$ (Table I) for all cellulose acetate membranes for which ln C^*_{NaCl}values are greater than −9.6. For such membranes, a constant value of ln Δ^* (= −0.92) can be assigned, and $D_{AM}/K\delta$ for the PEG solute can be calculated from eq. (6). Calculations based on eq. (6) showed that the value of ln C^*_{NaCl} for each film used remained essentially constant at the operating pressures of 50, 75, and 100 psig.

Further, for dilute feed solutions, eqs. (4) and (5) are applicable, and $PR \approx PWP$. Assuming that PWP is proportional to the operating gauge pressure up to 100 psig, the values of f were calculated using eqs. (4) to (6) for different PEG solutes with membranes of different surface porosities at the operating pressures of 50, 75, and 100 psig. The results obtained were in good agreement with the experimental data as shown in Table III, which illustrates the practical utility of the data given in Table II for the polar, steric, and nonpolar parameters and the predictability of reverse osmosis separations of PEG solutes in dilute aqueous solutions at low operating pressures.

Effect of Mass Transfer Coefficient and Operating Pressure on Solute Separation

The combined effect of operating pressure and mass transfer coefficient k on solute separation is particularly interesting in this work. Let v_s represent the permeation velocity (cm/sec) of product solution expression by

$$v_s = \frac{PR}{3600S\rho} \tag{16}$$

Equation (4) can be written as

$$D_{AM}/K\delta = v_s \left(\frac{1-f}{f}\right) \left[\exp\left(\frac{v_s}{k}\right)\right]^{-1} \tag{17}$$

or

$$\frac{1}{f} = 1 + \frac{(D_{AM}/K\delta)\exp(v_s/k)}{v_s} \tag{18}$$

At low operating pressures (P), v_s is proportional to P. Further, with reference to a given PEG solute, the value of $D_{AM}/K\delta$ for a given membrane may be assumed to be constant in the small operating pressure range of 25 to 100 psig on the basis of results given in Table III. At a given feed flow rate, the value of k for the PEG solute is given by eq. (5), which is independent of operating pressure. Consequently, at low operating pressures, both $D_{AM}/K\delta$ and k are independent of v_s. Differentiating eq. (18) with respect to v_s,

$$\frac{d}{dv_s}\left(\frac{1}{f}\right) = \left\{\frac{D_{AM}/K\delta}{v_s^2}\exp\left(\frac{v_s}{k}\right)\right\}\left(\frac{v_s}{k} - 1\right) \tag{19}$$

which becomes zero when $v_s/k = 1$. This means that a plot of $1/f$ versus v_s should pass through a minimum at $v_s/k = 1$. Since $v_s \propto P$, one would expect that with increase in operating pressure solute separation will tend to increase when v_s/k is less than 1 and decrease when v_s/k is greater than 1. This possibility, which has already been anticipated in the literature,[16] is explicitly illustrated by the experimental data obtained in this work as given in Figure 4.

Ultrafiltration and Reverse Osmosis

The practical distinction between ultrafiltration and reverse osmosis remains arbitrary.[17] The same mass transport and fluid mechanical factors have been shown to be relevant to both the processes.[18] Such relevance, however, does not differentiate between possible alternate mechanisms applicable for each of the

TABLE III
Comparison of Experimental and Calculated Solute Separations[a]

Solute	Film no.	Solute separation, % 50 psig Exptl.	50 psig Calcd.	75 psig Exptl.	75 psig Calcd.	100 psig Exptl.	100 psig Calcd.
PEG-200	1	40.1	42.7	43.9	47.0	46.9	49.6
	2	25.4	24.8	27.2	27.8	31.3	29.1
	3	22.8	23.8	25.4	26.1	29.2	26.9
	4	18.3	18.4	20.2	20.3	24.0	20.6
	5	11.7	13.5	13.2	14.1	14.6	13.4
PEG-300	1	53.5	55.5	58.2	59.3	62.1	61.0
	2	34.8	35.3	38.3	38.4	42.1	39.2
	3	33.7	34.0	36.7	36.1	40.0	36.2
	4	26.7	27.0	29.6	28.8	31.6	28.5
	5	16.0	20.0	17.4	20.2	20.0	18.5
PEG-400	1	66.3	63.6	67.0	66.8	70.4	67.9
	2	43.4	43.3	45.4	46.0	48.0	46.3
	3	41.3	41.7	43.3	43.5	45.9	42.9
	4	33.7	33.9	35.1	35.4	37.8	34.4
	5	19.9	25.5	20.6	25.1	23.5	22.5
PEG-600	1	75.0	72.3	75.8	74.5	77.7	74.9
	2	52.5	53.0	54.6	55.0	56.3	54.4
	3	51.0	51.1	52.5	52.2	54.4	50.5
	4	41.0	42.8	42.4	43.4	42.7	41.4
	5	27.0	32.7	26.3	31.3	27.2	27.2
PEG-1000	1	85.1	81.8	84.7	82.9	85.0	82.5
	2	67.2	65.7	66.3	66.5	66.3	64.9
	3	63.1	63.7	63.3	63.5	63.2	60.5
	4	53.9	55.5	53.1	54.7	52.7	51.1
	5	35.4	40.9	33.7	37.6	32.3	34.0
PEG-1500	1	90.7	88.0	90.0	88.2	89.7	87.3
	2	76.5	75.3	75.0	74.9	74.0	72.4
	3	72.1	73.3	72.0	72.0	70.2	67.7
	4	63.7	66.0	62.0	63.7	58.8	58.5
	5	45.1	50.7	41.0	45.4	37.5	39.0
PEG-4000	1	93.7	94.0	93.8	93.3	93.8	91.8
	2	86.4	85.8	83.7	83.9	82.7	79.9
	3	82.5	83.9	79.4	81.1	78.9	74.6
	4	76.2	78.4	71.6	73.9	69.2	65.7
	5	57.3	62.4	50.0	52.8	43.3	41.7
PEG-6000	1	97.1	97.1	95.8	96.4	95.2	94.6
	2	94.1	92.8	91.2	90.0	86.3	84.8
	3	90.2	91.2	87.5	87.5	81.7	78.5
	4	86.3	87.6	79.8	81.2	71.2	69.3
	5	70.6	73.7	59.6	62.1	42.3	38.4

[a] Solute concentration in feed, 50 ppm.

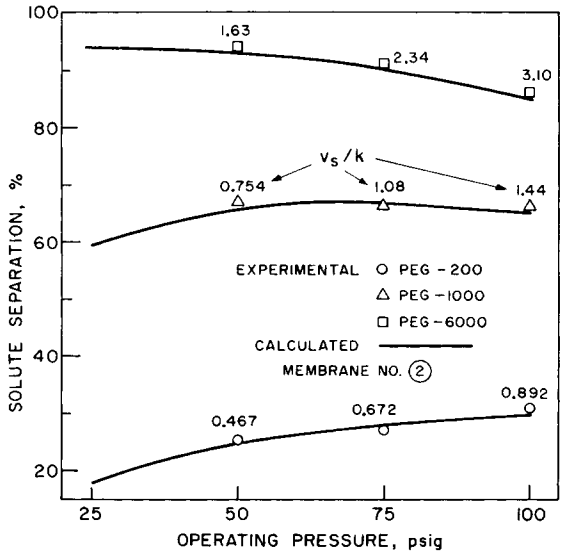

Fig. 4. Effect of operating pressure and v_s/k on solute separation.

above separation processes. Membrane separations of macromolecular solutes in aqueous solutions are conventionally treated as ultrafiltration, and the mechanism of such separation is implicitly or explicitly assumed to be just a mechanical sieving process. Such treatment of ultrafiltration experimental data generally involves the pregel- and gel-polarization phenomena, which may be reviewed briefly as follows.[18]

Because of the very low diffusivities of macromolecular solutes in aqueous solutions, especially at high concentrations, and the rheological properties of such solutions, the concentration polarization on the high-pressure side of the membrane during ultrafiltration results in the formation of a highly viscous non-Newtonian pregel fluid layer on the membrane surface. This layer, behaving like an additional membrane in series with the original membrane, offers significantly more resistance to hydraulic permeation than what can be accounted for on the basis of the osmotic pressure of the concentrated macromolecular solution constituting the pregel layer. At a certain limiting concentration, the above pregel layer transforms itself into a solid-like gel layer which is often visually identifiable as a slime or a cake on the membrane surface. This transformation occurs when the rate of convective transport of solute toward the membrane surface during ultrafiltration exceeds the diffusive back transport of solute from the membrane surface into the bulk solution. Once the above limiting concentration in the gel layer is reached, it remains constant, so that further buildup of solute due to concentration polarization during ultrafiltration occurs only by an increase in gel thickness.

The effects of pregel- and gel-polarization phenomena on solute separation and product rate are particularly evident in studies on the effects of increase in operating pressure on membrane performance during ultrafiltration. In the pregel-polarization region, with an increase in operating pressure, solute separation is decreased because of membrane permeation of the concentrated pregel fluid, and product rate is increased because of the increased driving force for fluid flow. The latter increase, however, is significantly less than proportional to the

increase in driving force based on concentration polarization alone because of the additional hydraulic resistance offered by the pregel layer. In the gel-polarization region, the product rate remains unchanged by an increase in operating pressure because the increaseed driving force is balanced by the increased resistance to fluid flow arising from the increased thickness of the gel layer. The effect of increase in operating pressure on solute separation in the gel-polarization region depends on the mechanical properties of the gel layer; if the solute concentration in the gel layer remains constant, an invariance in product rate should also result in an invariance in solute separation. All the above consequences of the pregel- and gel-polarization phenomena are consistent with the reported experimental ultrafiltration data.

The object of the foregoing review is to point out that none of the consequences of the pregel- and gel-polarization phenomena described above was evident in this work, and hence the treatment of experimental data on the basis of the above phenomena is neither admissible nor relevant to the data obtained in this work. The solute concentrations used in this work were extremely low; no slime or cake formation on the membrane surface could be identified at any time; the product rate was essentially the same as pure water permeation rate in all the experiments for all the membranes used; and, in each case, the product rate increased proportionately with increase in operating pressure. Consequently, there was absolutely no basis for assuming the occurrence of pregel or gel polarization on the high-pressure side of the membrane during the experiments.

On the other hand, both the product rate and solute separation data obtained in this work were characteristic of those normally obtained in reverse osmosis experiments involving nonionized organic solutes in aqueous solutions and preferential sorption of water at the membrane–solution interface.[5] This is reason enough to treat the data accordingly. Since reverse osmosis is a physicochemical process (and not a mechanical sieving process), the same physicochemical criteria applicable to the separation of monomeric nonionic organic solutes are also applicable for the separation of PEG solutes, which is the reason for the generation of the applicable polar, steric, and nonpolar parameters for the PEG solutes studied. This approach to the subject is further justified on the basis of the predictability of both solute separation and product rate data as illustrated in Table III and Figure 4.

Pregel- and gel-polarization phenomena can also occur in reverse osmosis systems involving macromolecular solutes in aqueous solutions and preferential sorption of water at the membrane–solution interface. In such cases, membrane performance (solute separation and product rate) would be controlled by the combined effects of the above phenomena and the polar, steric, and nonpolar forces prevailing at the membrane–solution interface. From a quantitative knowledge about the latter forces and the experimental reverse osmosis data for the above systems, it might be possible to characterize separately the resistances offered by the pregel and gel layers involved. This possibility offers an alternative approach to the conventional treatment of such membrane-separation data.

CONCLUSIONS

The concept of polar free-energy parameters governing reverse osmosis separations has been extended to polymer solutes. Methods have been developed for estimating both the steric and nonpolar parameters for polymer solutes. Using the data on polar ($-\Delta\Delta G/RT$), steric ($\delta^*\Sigma E_s$), and nonpolar ($\omega^*\Sigma s^*$) parameters generated in this work for PEG solutes, values of ln C^*_{NaCl} representing surface pore structure can be obtained for cellulose acetate membranes using an appropriate PEG solute as the reference solute. Thus this work offers a means of characterizing cellulose acetate membranes whose surface pores are too big for significant separation of NaCl under reverse osmosis experimental conditions.

This paper also demonstrates that solute separation in reverse osmosis does not always have to increase with increase in operating pressure even when water is preferentially sorbed at the membrane-solution interface; depending on operating conditions, solute separation can increase or decrease with increase in operating pressure as predicted by the basic transport equations governing reverse osmosis.[12]

One of the authors (F.H.) thanks the National Research Council of Canada for the award of a postdoctoral associateship, issued as N.R.C. No. 17021.

References

1. T. Matsuura and S. Sourirajan, *J. Appl. Polym. Sci.*, **16,** 1663 (1972).
2. T. Matsuura and S. Sourirajan, *J. Appl. Polym. Sci.*, **17,** 1043 (1973).
3. S. Sourirajan and T. Matsuura, in *Reverse Osmosis and Synthetic Membranes,* S. Sourirajan, Ed., National Research Council Canada, Ottawa, 1977, Chap. 2.
4. T. Matsuura, M. E. Bednas, J. M. Dickson, and S. Sourirajan, *J. Appl. Polym. Sci.*, **18,** 2829 (1974).
5. T. Matsuura, J. M. Dickson, and S. Sourirajan, *Ind. Eng. Chem., Process Des. Dev.*, **15,** 149 (1976).
6. T. Matsuura, A. G. Baxter, and S. Sourirajan, *Ind. Eng. Chem., Process Des. Dev.*, **16,** 82 (1977).
7. O. Kutowy, W. L. Thayer, and S. Sourirajan, *Desalination,* **26,** 195 (1978).
8. S. Sourirajan, *Reverse Osmosis,* Academic, New York, 1970, Chap. 3.
9. H. Fujita, in *Encyclopedia of Polymer Science and Technology,* Vol. 5, N. M. Bikales, Ed., Interscience, New York, 1966, pp. 65–82.
10. A. Einstein, *Ann. Phys.*, **17,** 549 (1905).
11. L. Mandelkern and P. J. Flory, *J. Chem. Phys.*, **20**(2), 212 (1952).
12. S. Sourirajan and T. Matsuura, in *Reverse Osmosis and Synthetic Membranes,* S. Sourirajan, Ed., National Research Council Canada, Ottawa, 1977, Chap. 3.
13. T. Matsuura and S. Sourirajan, *Ind. Eng. Chem., Process Des. Dev.*, **10,** 102 (1971).
14. T. Matsuura, L. Pageau, and S. Sourirajan, *J. Appl. Polym. Sci.*, **19,** 179 (1975).
15. T. Matsuura and S. Sourirajan, *J. Appl. Polym. Sci.*, **17,** 3683 (1973).
16. T. Matsuura, M. E. Bednas, and S. Sourirajan, *J. Appl. Polym. Sci.*, **18,** 567 (1974).
17. A. S. Michaels, in *Progress in Separation and Purification,* Vol. 1, E. S. Perry, Ed., Interscience, New York, 1968, p. 297–334.
18. W. F. Blatt, A. Dravid, A. S. Michaels, and L. Nelson, in *Membrane Science and Technology,* J. E. Flinn, Ed., Plenum, New York, 1970, pp. 47–97.

Received October 11, 1977
Revised November 30, 1977